Cancer Research

Pancreatic Ductal Adenocarcinoma Mice Lacking Mucin 1 Have a Profound Defect in Tumor Growth and Metastasis

Dahlia M. Besmer[1], Jennifer M. Curry[1], Lopamudra D. Roy[1], Teresa L. Tinder[1], Mahnaz Sahraei[1], Jorge Schettini[1], Sun-Il Hwang[2], Yong Y. Lee[2], Sandra J. Gendler[3], and Pinku Mukherjee[1]

Abstract

MUC1 is overexpressed and aberrantly glycosylated in more than 60% of pancreatic ductal adenocarcinomas. The functional role of MUC1 in pancreatic cancer has yet to be fully elucidated due to a dearth of appropriate models. In this study, we have generated mouse models that spontaneously develop pancreatic ductal adenocarcinoma (KC), which are either Muc1-null (KCKO) or express human MUC1 (KCM). We show that KCKO mice have significantly slower tumor progression and rates of secondary metastasis, compared with both KC and KCM. Cell lines derived from KCKO tumors have significantly less tumorigenic capacity compared with cells from KCM tumors. Therefore, mice with KCKO tumors had a significant survival benefit compared with mice with KCM tumors. *In vitro*, KCKO cells have reduced proliferation and invasion and failed to respond to epidermal growth factor, platelet-derived growth factor, or matrix metalloproteinase 9. Further, significantly less KCKO cells entered the G_2–M phase of the cell cycle compared with the KCM cells. Proteomics and Western blotting analysis revealed a complete loss of cdc-25c expression, phosphorylation of mitogen-activated protein kinase (MAPK), as well as a significant decrease in nestin and tubulin-α2 chain expression in KCKO cells. Treatment with a MEK1/2 inhibitor, U0126, abrogated the enhanced proliferation of the KCM cells but had minimal effect on KCKO cells, suggesting that MUC1 is necessary for MAPK activity and oncogenic signaling. This is the first study to utilize a Muc1-null PDA mouse to fully elucidate the oncogenic role of MUC1, both *in vivo* and *in vitro*. *Cancer Res; 71(13); 4432–42. ©2011 AACR.*

Introduction

Pancreatic ductal adenocarcinoma (PDA) is the fourth leading cause of cancer-related deaths in the United States (1). It is one of the most deadly cancers due to its aggressive nature and relatively few treatment options. With a 5-year survival rate of only 5%, it has the poorest prognosis among all cancers. To date, the only potential curative is surgical resection, of which only 20% of patients are eligible. Alternative therapies, such as radiotherapy and chemotherapy remain largely ineffective. The development and evaluation of novel targeted therapeutic agents for improving the outcome of patients are of paramount importance.

Importantly, MUC1 is a membrane-tethered mucin glycoprotein expressed on the apical surfaces of normal glandular epithelia but is overexpressed and aberrantly glycosylated in more than 60% of human PDA and in 100% of metastatic lesions (2, 3). In human cancers, MUC1 is commonly detected in high-grade, but not in low-grade, pancreatic intraepithelial neoplasia (PanIN; refs. 4, 5). Thus, MUC1 may play an important role in the development and progression of PDA (6–8). Overexpression of MUC1 in pancreatic cancer has been known for quite some time; however, its function has not been clearly elucidated, mainly due to the lack of an appropriate pancreatic cancer model.

Activating mutations in the *KRAS* proto-oncogene are found in more than 90% of invasive PDA and are thought to represent an initiating event. Recently, a transgenic mouse model has been created that expresses physiologic levels of oncogenic KRAS with a glycine to aspartate substitution at codon 12 in the progenitor cells of mouse pancreas (9). These mice, designated as KC or Cre-LSL-$KRAS^{G12D}$, develop the full spectrum of PDA. We have further crossed the KC mice to the human MUC1 transgenic (MUC1.Tg) mice which express MUC1 in a pattern and level consistent with that in humans (designated KCM; ref. 3). KC mice were also crossed with the Muc1KO mice (designated KCKO), creating a Muc1-null PDA model. These mouse models provide us with a unique opportunity to fully evaluate the role of MUC1 in pancreatic cancer development.

This study is the first to utilize a model of pancreatic cancer that is Muc1-null to fully elucidate the oncogenic role of MUC1. In this study we show that lack of Muc1 significantly

Authors' Affiliations: [1]Department of Biology, University of North Carolina; [2]Department of Proteomics, Carolinas Health Care Center, Charlotte, North Carolina; and [3]Department of Biochemistry and Molecular Biology, Mayo Clinic Arizona, Scottsdale, Arizona

Note: Supplementary data for this article are available at Cancer Research Online (http://cancerres.aacrjournals.org/).

Corresponding Author: Pinku Mukherjee, Department of Biology, University of North Carolina-Charlotte, 9201 University City Blvd, Charlotte, NC 28223. Phone: 704-687-5459; Fax: 704-687-3122; E-mail: pmukherj@uncc.edu

doi: 10.1158/0008-5472.CAN-10-4439

decreased proliferation, invasion, and mitotic rates both *in vivo* and *in vitro*. Importantly, treatment with MAP/ERK kinase 1/2 (MEK1/2) inhibitor, U0126, completely abrogated the enhanced proliferation of the KCM cells. These data therefore may have implications in the future design of MUC1-targeted therapies for pancreatic cancer.

Materials and Methods

Spontaneous mouse models and tissue culture

KC mice were generated in our laboratory on the C57BL/6 background by mating the P48-Cre with the LSL-KRASG12D mice (10, 11). They were further mated to the MUC1.Tg mice to generate KCM mice (3, 12) or to the Muc1KO mice (13) to generate KCKO mice. Tumors were excised at predetermined time points and weighed. Gross metastasis was evaluated in the lung, liver, and peritoneum. Tumors were dissociated by using collagenase IV (Worthington Biochemical) and cell lines generated in our laboratory. Cell lines are designated KCKO for those cells lacking Muc1 and KCM for those cells expressing MUC1. As we have been unable to generate the KC cell lines, we have compared KCM with KCKO. The cells were maintained in complete Dulbecco's modified Eagle's medium (Invitrogen) supplemented with 10% FBS (HyClone), 1% glutamax (Invitrogen), and 1% penicillin/streptomycin.

ELISA

Prostaglandin E_2 (PGE_2) levels in the tumor lysate were determined by a specific ELISA kit for PGE_2 metabolite (PGE-M; Cayman Pharmaceuticals). VEGF levels were also determined by specific ELISA (RayBiotech).

^{3}H-thymidine incorporation

KCM and KCKO cells were serum-starved for 24 hours and treated for 30 minutes with rm-PDGF-CC (Peprotech), rm-EGF (Peprotech), and rm-MMP9 (R&D systems) at a concentration of 50 ng/mL, or MEK1/2 inhibitor at 10 μmol/L concentration. Cell proliferation was determined by using [^{3}H]-thymidine incorporation, in which 1 μCi of [^{3}H]-thymidine was added per well for 24 hours before harvesting. Incorporated thymidine was evaluated by using the Topcount microscintillation counter. All determinations were carried out in triplicate.

CFSE dilution assay

Cells were stained by using the CellTrace CFSE Kit (Molecular Probes). Carboxyfluorescein succinimidyl ester (CFSE) was added to the cells at a final concentration of 2 μmol/L, incubated for 15 minutes at 37°C, and 0.5×10^6 cells removed for initial positive staining. The remaining cells were plated in triplicate. Cells were harvested at predetermined time points and CFSE dilution was determined by flow cytometry (Beckman Coulter). Analysis was carried out by using FlowJo (Treestar).

Cell-cycle analysis

Cells were harvested, fixed by resuspending in 10 mL of 70% ethanol for 30 minutes, and washed in ice-cold PBS. The pellets were resuspended in 0.5 mL PBS, and 1 mL of DNA extraction buffer was added. Cells were incubated, washed, and resuspended in DNA staining solution containing 20 μg/mL propidium iodide (PI; Sigma-Aldrich) and 100 μg/mL RNase (Invitrogen). DNA content was determined by flow cytometry and analyzed by FlowJo.

Invasion assays

Cells (serum starved for 24 hours) were treated with rm-PDGF, rm-EGF, or rm-MMP-9 for 30 minutes, trypsinized, washed, and resuspended in Serum Free Media (SFM). Cells were plated over transwell inserts (BD Biosciences) precoated with growth factor–reduced Matrigel (BD Biosciences), and permitted to invade toward serum contained in the bottom chamber for 48 hours. Percent invasion was determined as described in ref. 14.

Western blots and proteomics

Western blotting was carried out as previously published (14). MUC1 CT antibody CT2, was made in Mayo Clinic Immunology Core (14). MUC1 TR antibody was provided by Dr. Joyce Taylor-Papadimitriou. ERK1/2 antibodies, phospho-p44/42 and p44/42, were purchased from Cell Signaling Technologies. All other antibodies (p53, CDKN1A, c-myc, TGFβ-R1, MEK1, Cyclin B1, Wee 1, Cdc2-p34, Cdc-25c, and β-actin) were purchased from Santa Cruz Biotechnologies and used according to manufacturer's recommendations. Proteomics analysis was determined as previously described (14).

In vivo tumor growth

Ten–week- and 9-month-old mice were injected with 1×10^6 KCM or KCKO cells (in 50 μL of PBS combined with 50 μL of growth factor–reduced Matrigel) into the flank of the mice ($n = 8$). Mice were palpated starting at 6 days post–tumor injection. Tumor weight was calculated according to the formula: weight in grams = [length in centimeters × (width in centimeters)^2]/2 (14). Upon sacrifice, the tumors were weighed, prepared for lysates, and fixed for immunohistochemistry (IHC).

Hematoxylin and eosin staining

Tissues were fixed in 10% neutral-buffered formalin. Paraffin-embedded blocks were prepared by the Histology Core at The Mayo Clinic and 4-μm thick sections were cut for staining. Slides were hematoxylin and eosin (H&E) stained, and images taken at ×100 and ×200 magnifications.

Statistical analysis

Data were analyzed by using GraphPad software. Results are expressed as mean ± SEM and are representative of greater than or equal to 3 separate experiments. Comparison of groups was done by using 1-way or 2-way ANOVA followed by the Bonferroni posttest for multiple comparisons (*, $P < 0.05$, **, $P < 0.01$, ***, $P < 0.001$).

Results

In the absence of Muc1, pancreatic tumor burden and secondary metastasis are decreased

Mice were sacrificed at 6, 16, 26, and 40 weeks of age. The pancreas weight was used as the indicator of tumor weight. At

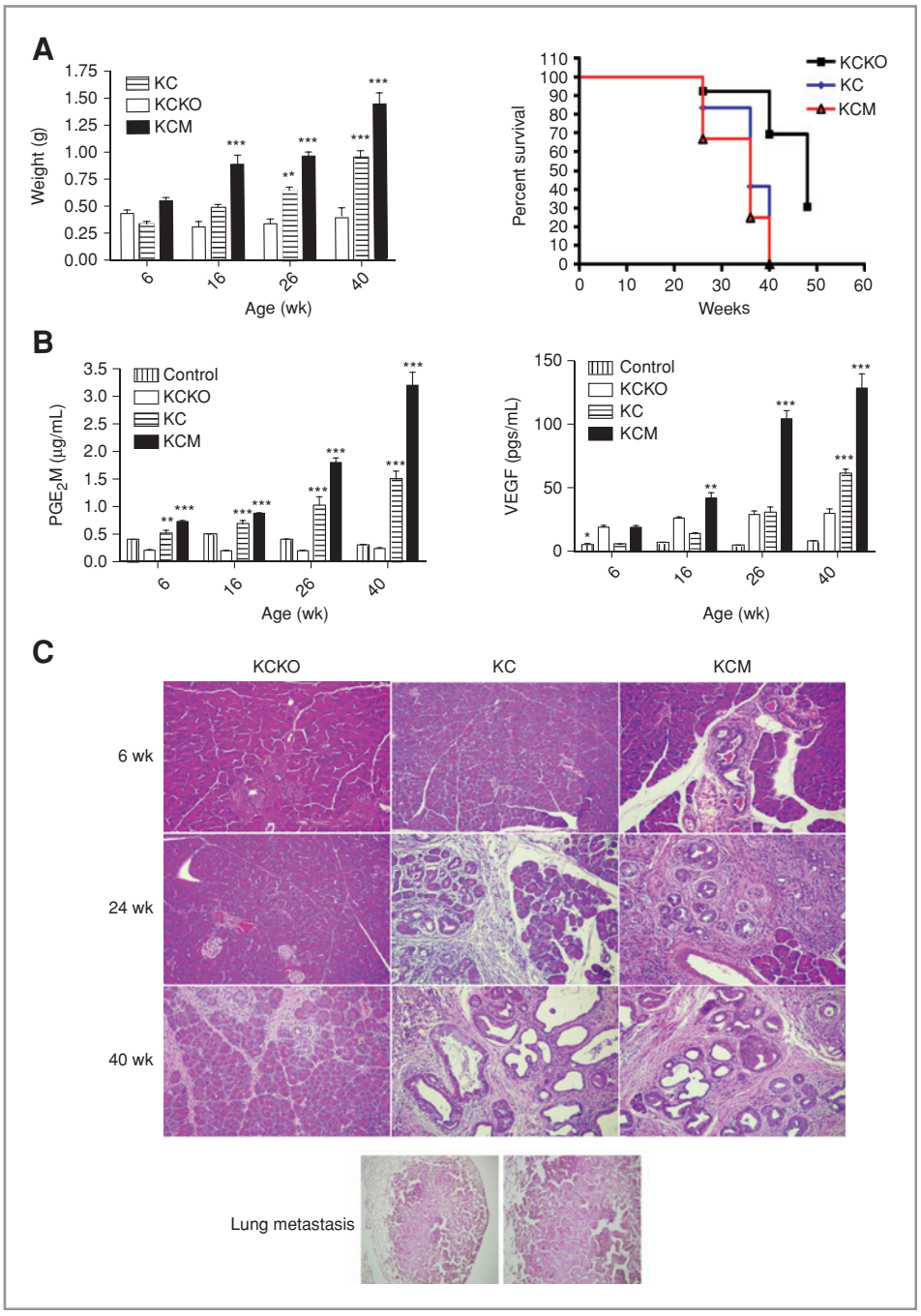

Figure 1. KCKO mice have lower tumor burden, metastasis, and levels of VEGF and PGE_2 with higher survival rate compared with KC and KCM mice. A, pancreas weight and survival of KCKO, KC, and KCM mice. Pancreas weight: **, $P < 0.01$; ***, $P < 0.001$ compared with KCKO; survival: *, $P < 0.01$ compared with KCM and KC. B, circulating levels of PGE_2-M and VEGF in C57Bl/6, KCKO, KC, and KCM mice. **, $P < 0.01$; ***, $P < 0.001$ compared with KCKO. C, representative IHC images of pancreas from KCKO, KC, and KCM mice as a function of age (×200). Representative H&E of lung metastasis (×100 and ×200).

6 weeks of age, there was no statistical difference between KCKO and either KC or KCM. However, by 16 weeks of age and thereafter, KC and KCM mice had significantly higher tumor burden than KCKO mice (Fig. 1A). It must be noted that the KCM mice had significantly higher tumor burden than KC mice confirming our previous results that overexpression of MUC1 augments pancreatic tumor progression (3). Most importantly, pancreas weight did not increase from the age of 6 to 40 weeks in mice lacking Muc1 suggestive of a stable disease (Fig. 1A). Further, KCKO mice showed a significant survival benefit compared with the KC and KCM mice (Fig. 1A).

We have previously shown that MUC1-expressing PDA have higher levels of VEGF and PGE-M (3), leading to higher angiogenesis and metastasis (15). Therefore, we evaluated the circulating levels by specific ELISA. Both VEGF and PGE-M levels were significantly lower in the KCKO mice than the KC and KCM mice, and most notably the levels did not

increase with age in the KCKO mice as noted in KC and KCM mice (Fig. 1B). PGE_2 is an end product of the COX-2 pathway and is known to induce tumor cell proliferation and increase motility (16, 17).

H&E-stained pancreas sections were examined from 6-, 24-, and 40-week-old KC, KCM, and KCKO mice. Clearly, abnormal duct with low grade PanIN lesions were visualized in the KCM pancreas as early as 6 weeks of age (Fig. 1C). At this time point, the pancreas from KC and KCKO mice looked relatively normal. By 24 and 40 weeks of age, both KC and KCM pancreas showed PanIN lesions of varying grades with KCM pancreas showing signs of higher grade PanIN lesions and adenocarcinoma (Fig. 1C). These data confirm our previously published analysis of the PanIN lesions in KC and KCM pancreas as a function of age (3). Most notably, pancreas from KCKO mice did not show high-grade PanIN lesions even at 24 and 40 weeks of age (Fig. 1C). The data from these spontaneous models clearly point toward the critical role of MUC1 in the progression of pancreatic cancer. Further, pancreas sections from 26-week-old KCM mice showed increased expression of VEGF, matrix metalloproteinase 9 (MMP9), epidermal growth factor receptor (EGFR), and platelet derived growth factor (PDGF) as compared with age-matched KC and KCKO pancreas (Supplementary Fig. S1). Data show the highly aggressive nature of MUC1-expressing tumors which is substantiated by increased proliferating cell nuclear antigen staining in KCM and KC pancreas as compared with the KCKO pancreas (data not shown).

At 36 to 40 weeks of age, mice were euthanized and lungs, liver, and peritoneum were evaluated for macroscopic gross lesions. Interestingly, 61% of KCM mice developed lung metastasis, 33% developed liver metastasis, and 23% developed peritoneal metastasis ($n = 13$). This is in stark contrast to the KCKO mice which had merely 10% of mice develop metastasis in any of the 3 organs ($n = 10$). Thirty percent of the KC mice ($n = 13$) had developed lung metastasis, 20% had developed liver metastasis, and 10% had developed peritoneal metastasis. As an example, a representative H&E image of a lung showing clear metastatic lesion is provided in Figure 1C.

Muc1-null tumor cells have significantly lower tumorigenic capacity than their MUC1-expressing counterpart

To further decipher the underlying mechanism of enhanced proliferation and progression in MUC1-expressing tumors, we generated several cell lines from the KCM and KCKO tumors and first studied their tumor forming ability *in vivo* in both young and old mice. In the 8- to 10-week-old mice ($n = 4$), both cell lines formed palpable tumors by 6 days postinjection. By 12 days post–tumor challenge, KCM tumors grew faster ($P < 0.001$), and continued the same trend until sacrifice at 21 days postinjection (Fig. 2A). By day 21, the tumor burden in mice injected with KCM ($n = 5$), as determined by caliper measurement, had grown to an average of 1,017 mg, whereas the mice injected with KCKO had a tumor burden of merely 461 mg ($n = 6$). During necropsy, tumors were excised and weighed. KCM tumors weighed on an average of 700 mg whereas KCKO remained at 500 mg (Fig. 2A).

Because the median age of pancreatic cancer patients is more than 65 years, we assessed whether this observation would hold true in aged mice. In 9-month-old mice (Fig. 2B; $n = 5$ mice per group), tumor burden was again significantly higher, with KCM versus KCKO cells starting at 12 days postinjection ($P < 0.05$) and continued until 21 days reaching a tumor weight of 1,300 mg for KCM versus 300 mg for KCKO (Fig. 2B). It must be noted that in the aged mice, the KCM cells grew more aggressively than in the younger mice and reached a much higher tumor burden at day 21 (compare Fig. 2A and B), but KCKO growth remained consistent.

Survival is significantly higher in mice injected with pancreatic cancer cells lacking MUC1

To assess survival, mice were injected with KCM and KCKO cells and tumors were allowed to grow until reaching 10% of the body weight or until ulcerations developed, whichever came first (Fig. 2C). Survival was significantly increased in mice injected with KCKO compared with KCM cells ($P < 0.001$). By 25 days post–tumor challenge, none of the mice injected with KCM cells survived ($n = 7$), whereas 100% of mice injected with KCKO cells ($n = 6$) survived at that age (Fig. 2C). Mice injected with KCKO survived until approximately 40 days post–tumor injection. Tumor weight, derived from caliper measurements, shows a steady growth rate of tumors injected with KCM, whereas the KCKO tumor growth remains stunted and does not exceed 500 mg (Fig. 2D). These data recapitulate the data from the spontaneous model of PDA in Figure 1.

Cell division and cell-cycle progression is significantly altered in pancreatic cancer cells lacking Muc1/MUC1

To further analyze the effects of MUC1 on the *in vitro* kinetics of cellular division, KCKO and KCM were subjected to the CFSE dilution assay, which fluorescently labels cells and is depleted as they divide. Initial staining of KCM cells with CFSE resulted in a mean fluorescence intensity (MFI) of 2,499. After 48 hours, CFSE had already been diluted to an MFI of 96. Initial staining of KCKO cells resulted in an MFI of 1,500. After 48 hours, CFSE had been diluted to an MFI of 73 (Fig. 3A). Although the KCM cells initially stained with greater intensity than did the KCKO cells, the CFSE was diluted much faster as can be seen by the slope of the line displaying MFI dilution over time (Fig. 3B).

As we observed that MUC1 affects cell division, we next investigated how the cell cycle was affected by MUC1 expression. Cells were stained with PI and the DNA content was determined by flow cytometry. KCM cells progress through the cell cycle at a steady rate. At 12 hours postplating, 26.9% of KCM cells were in the G_0–G_1, 34.3% in S, and 32.5% in G_2–M phases of the cell cycle (Fig. 3C). In contrast, KCKO cells that lack Muc1 had a significantly different distribution at both 12- and 24-hour time points ($P < 0.001$; Fig. 3D). At 12 hours postplating, KCKO cells had 31.1% of cells in G_0–G_1,

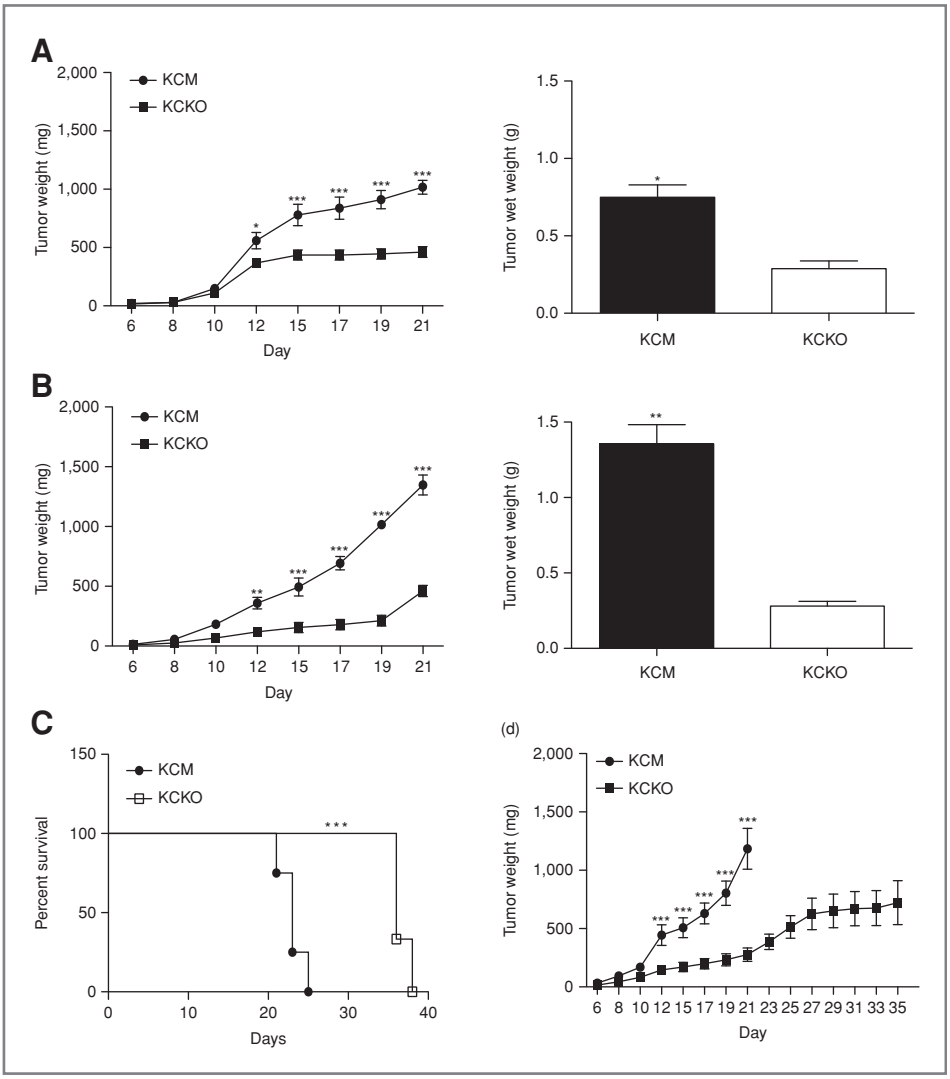

Figure 2. Significantly decreased tumor burden and increased survival in syngeneic C57/BL6 mice challenged with KCKO versus KCM cells. A, tumor growth curve and tumor wet weight in 8- to 10-week- and 9-month-old mice. Significantly higher tumor weight in mice injected with KCM versus KCKO cells. *, $P < 0.05$; ***, $P < 0.001$. B, tumor growth curve and tumor wet weight in 9-month-old mice. Significantly higher tumor weight in mice injected with KCM versus KCKO cells. **, $P < 0.01$; ***, $P < 0.001$. C, survival curve of 8- to 10-week-old mice challenged with KCKO and KCM cells. Significantly higher survival rate in mice injected with KCKO versus KCM tumors. ***, $P < 0.001$. D, tumor growth curve of KCM versus KCKO cells of mice in the survival study. ***, $P < 0.001$.

52.9% in S, and 13.3% of cells in G_2–M phases. This distribution remained relatively similar, in both cell types by 24 hours postplating (Fig. 3C). KCKO cells clearly enter and accumulate in the S-phase where the DNA doubling occurs more rapidly than KCM cells, but thereafter KCKO cells do not progress to the G_2 and mitotic phases as efficiently as KCM cells.

KCKO cells fail to proliferate or invade in response to EGF, PDGF, and MMP9

To assess whether KCKO cells would respond to growth factors known to induce cell division, proliferation, and invasion of cancer cells, KCKO and KCM cells were subjected to an *in vitro* proliferation assay, as determined by [^{3}H]-thymidine uptake. First, KCM cells displayed a significantly higher rate of proliferation compared with KCKO cells. Stimulation with EGF, PDGF, or MMP9, did not induce proliferation in KCKO cells (Fig. 4A–C). With regards to invasion, the basal level invasion index of the KCKO cells was found to be significantly lower than KCM cells (Fig. 4D; $P < 0.001$). More importantly, KCKO cells did not respond to any of the exogenous factors to increase its invasion index (Fig. 4D), and neither did the KCM cells, which could be because of the high basal invasion index. Altogether, the data suggest a failure of the KCKO cells to respond to exogenous EGF, PDGF, or MMP.

Complete loss of cdc-25c expression and decreased phosphorylation of mitogen-activated protein kinase in KCKO cells may account for lower mitosis, proliferation, and invasion

Once it was confirmed that cell-cycle progression and proliferation was altered in cells lacking MUC1, we began to investigate what specific proteins and markers were altered to cause such drastic differences. KCKO and KCM cells were subjected to both Western blot analysis and proteomics. We probed for those proteins typically involved in cell-cycle regulation pathways. Most notable was the complete loss of the tumor suppressor proteins, p53 and downstream p21, in

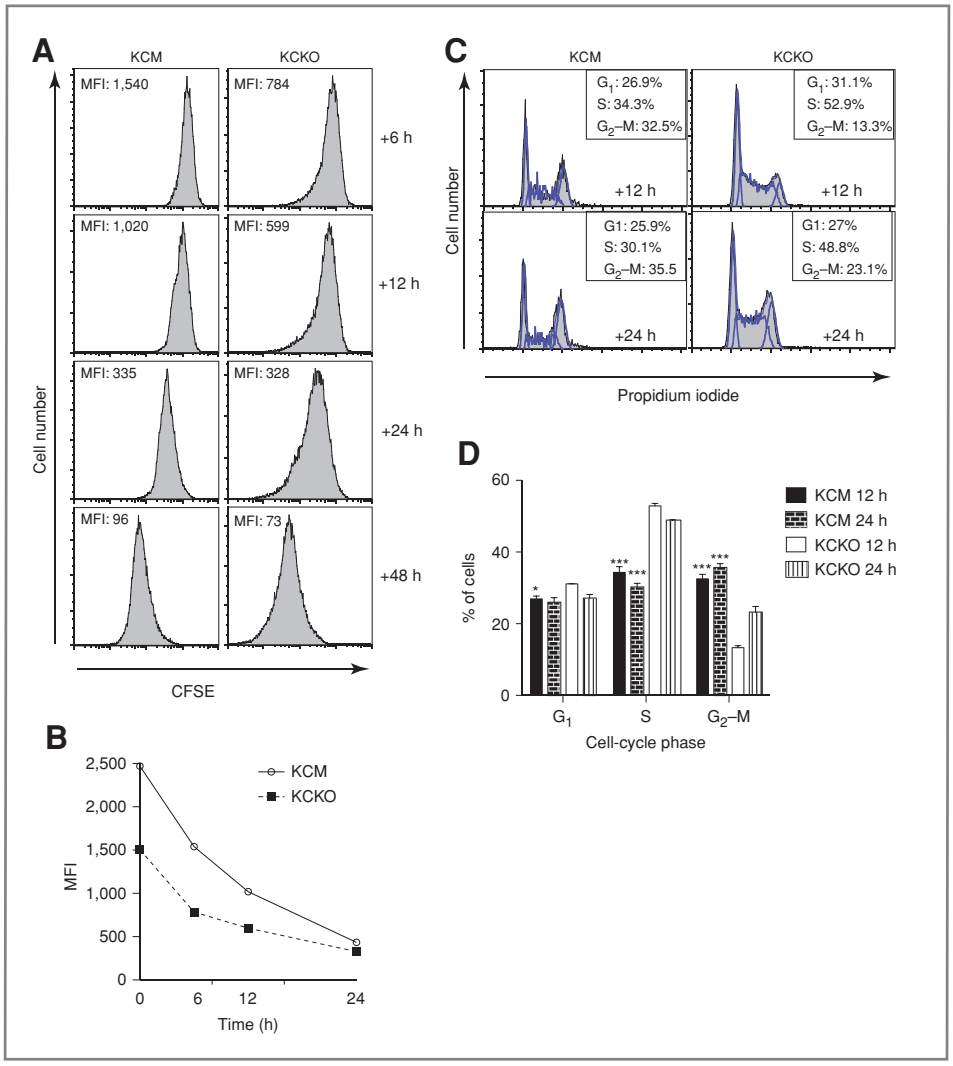

Figure 3. Significantly altered rate of cell division and progression through the cell cycle in KCKO versus KCM cells. A, CFSE staining in KCM and KCKO cells by flow cytometry. At time zero, KCM cells had MFI of 2,499, by 48 hours, CFSE had been diluted to an MFI of 96. In KCKO cells, the initial MFI was 1,500, whereas by 48 hours, CFSE had been diluted to MFI of 73. B, average MFI of CFSE staining in KCM and KCKO cells as a function of time in 3 experiments. C, cell-cycle analysis of KCM and KCKO cells by flow cytometry at 12 and 24 hours. D, percentage of KCM and KCKO cells in the G_0–G_1, S, and G_2–M phases of the cell cycle. Average of 3 experiments is shown.

the KCM cells but not in the KCKO cells. Associated with this was the complete loss of the M-phase inducer phosphatase, cdc-25c, in the KCKO cells (Fig. 5A). Furthermore, there was a significant downregulation of levels of phosphorylated mitogen-activated protein kinase (MAPK) p44/42 in the KCKO cells compared the KCM cells (Fig. 5A). Cdc-25c is a tyrosine phosphatase that directs dephosphorylation of cyclin B–bound CDC2 and triggers entry into mitosis. Thus, it becomes plausible to speculate that KCKO cells do not enter the mitotic phase efficiently because of the absence of Cdc-25c expression. Cdc-25c is also known to suppress p53-induced growth arrest, which possibly explains why cells lacking Cdc25-c and lacking Muc1 do not lose p53 and p21 expression, do not phosphorylate MAPK, and therefore do not divide, proliferate, and invade effectively.

MUC1 increases expression of tubulin-α2 chain and nestin protein

These alterations in cell-cycle regulation were coupled with differential transcription of genes associated with proliferation and metastasis. Proteomics analyses of a total of 2,874 cancer progression–associated proteins showed downregulation of 757 proteins in KCKO versus KCM cells. Genes with a decrease 2-fold and less were considered to be significant and are shown in Figure 5B. It is extremely relevant that the most pronounced downregulation was seen in tubulin-α2 chain and nestin in KCKO cells, and therefore these proteins were highly upregulated in KCM cells (Fig. 5B). Tubulin-α2 is a major constituent of microtubules and is required for mitotic spindle organization, mitosis, growth, and cell migration. Similarly, nestin is a marker of proliferating and migrating cells and highly expressed in mitotically active cells.

Treatment with MEK1/2 inhibitor, U0126, completely abrogates the enhanced proliferation in KCM cells

As MEK1 phosphorylation is a critical signaling event for proliferation of KCM cells, we treated KCKO and KCM cells with U0126. As a positive control, cells were treated with 20% FBS. As was expected, the basal level of activated MEK1 was

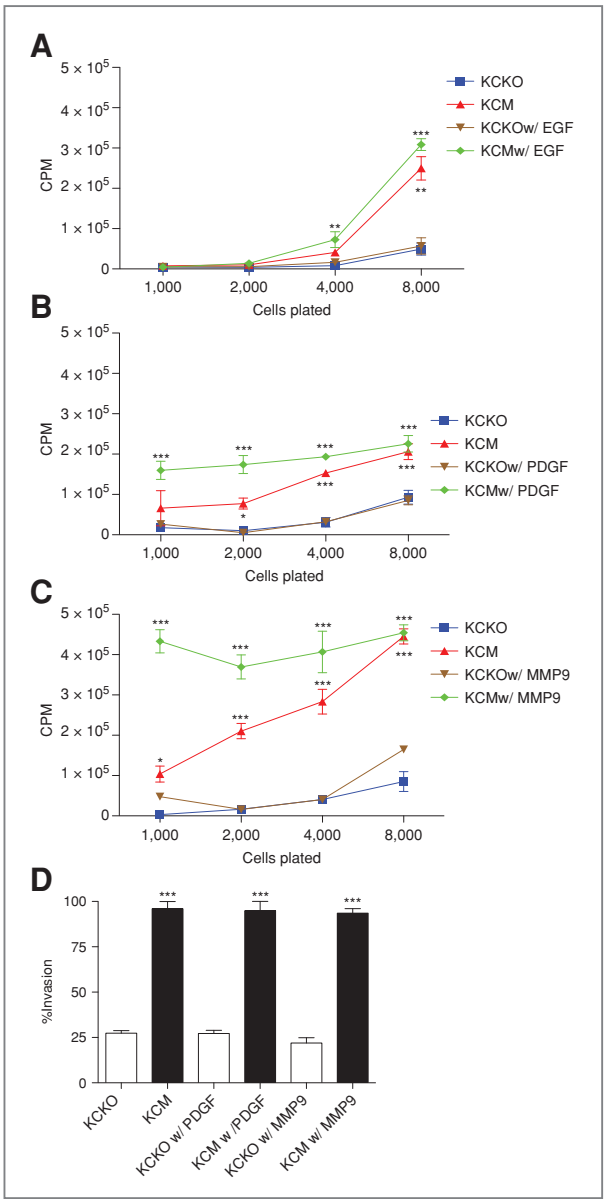

Figure 4. Significantly lower proliferation and invasion index in KCKO versus KCM cells. A–C, proliferation as measured by [^{3}H]-thymidine uptake in response to EGF (A), PDGF (B), and MMP9 (C). Significantly higher proliferation was observed in KCM versus KCKO cells. *, $P < 0.05$; ***, $P < 0.001$. D, percentage of KCM and KCKO cells that invaded in response to PDGF and MMP9. ***, $P < 0.001$.

higher in KCM cells than in KCKO cells (Fig. 6A). Similar to the cell lines, lysates from primary tumors of 26-week-old KCKO mice showed reduced phosphorylation of MAPK versus tumors from the KCM mice (Fig. 6A). This confirmed that activated MEK is a function of MUC1 expression and is critical in the progression of pancreatic cancer. When cell lines were treated with U0126, activation of MEK1/2 was completely abolished (Fig. 6A). To assess whether MEK1/2 is responsible for MUC1-enhanced cellular division and proliferation, KCM and KCKO cells treated with U0126 were subjected to CFSE dilution and [^{3}H]-thymidine uptake assays. CFSE dilution assay results are displayed as change in MFI at 6, 12, and 24 hours (Fig. 6B). Within 6 hours, KCM cells have already undergone rapid cell division as compared with KCKO cells (Fig. 6B; $P < 0.001$) and treatment with the inhibitor did not significantly reduce cell division in either cell lines. However, at 12 hours and 24 hours posttreatment, cell division was significantly less in KCM cells with treatment ($P < 0.001$ as compared with basal cell division) but there was no significant change in the KCKO cells with U0126 treatment (Fig. 6B). Both sets of cells supplemented with 20% FBS have significantly increased cell division albeit KCM always showed significantly rapid cell division compared with KCKO cells ($P < 0.001$, Fig. 6B). It is noteworthy that addition of the MEK1/2 inhibitor reduced cell division of the KCM cells to the level of KCKO cells at all time points.

Similar results were obtained by using the [^{3}H]-thymidine uptake assay. At 6 and 12 hours posttreatment with U0126, proliferation of KCM cells was significantly decreased from its basal level proliferation (Fig. 6C; $P < 0.001$) and reached the level of KCKO cells. At 24 hours after treatment, there was no statistical significance between KCKO treated with U0126 and KCM treated with U0126. KCKO, on the contrary, did not respond to the inhibitor such that the basal proliferation and inhibitor-treated proliferation remained similar suggesting that these cells do not require MEK1 activation. As expected, KCM cells were significantly more proliferative than KCKO cells ($P < 0.001$) at all time points.

Discussion

MUC1 is aberrantly overexpressed in pancreatic cancer (8). Overexpression of MUC1 is detectable during the early stages of pancreatic cancer development and is further increased in invasive carcinoma in humans and mice (3, 4). However, it is not known whether pancreatic cancer cells are dependent on MUC1 for their growth and survival. Using appropriate mouse models, we show unequivocally for the first time that pancreatic cancer cells depend on MUC1 to grow and survive, by directly suppressing p53 and its major transcriptional target p21Cip (Fig. 5) while activating MAPK, cdc-25-c, tubulin-α2, and nestin (Fig. 5). This in turn stimulates proliferation and mitosis (Figs. 3 and 4). Further, for survival, MUC1 expression causes the upregulation of several multidrug resistance proteins and prosurvival factors that protect them from undergoing apoptosis (Fig. 5). This is in stark contrast to what occurs in Muc1-null cells, in which the oncogenic signaling is shut down even though the *KRas* oncogene remains active. Muc1 deficiency leads to the failure to form tumors *in vivo* (Fig. 2) and decreased proliferation and invasion (Figs. 1–4).

The first evidence that MUC1 is required for pancreatic tumor growth came from the observation that the tumor weight of pancreas remained unchanged between 6 and 40 weeks of age in Muc1-null mice, whereas, the tumor weight increased significantly in wild-type mice (Fig. 1A). This lack of tumor growth in the Muc1-null mice was further substantiated when cell lines generated from tumors in these mice resulted in stable disease when injected *in vivo* (Fig. 2A–D) and

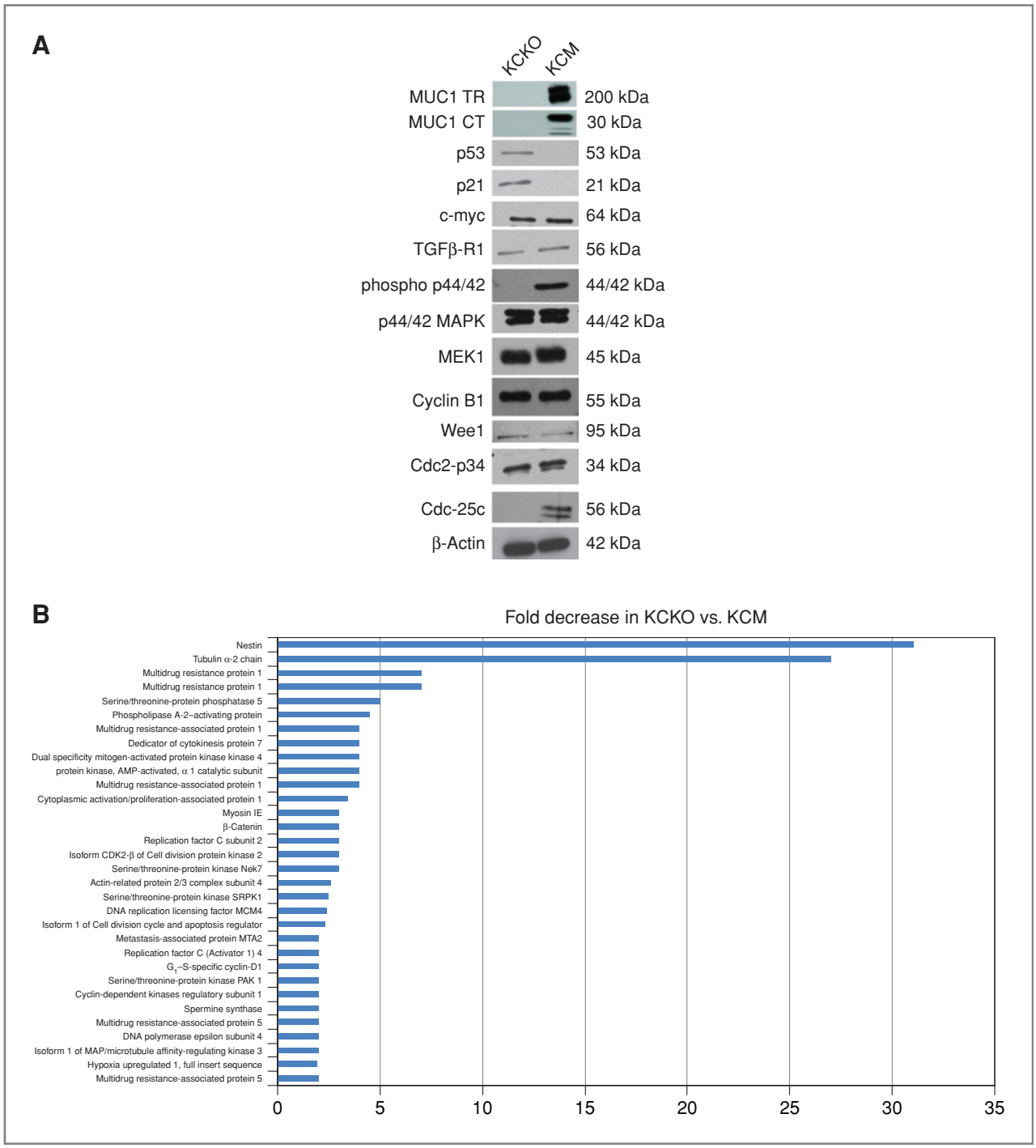

Figure 5. Differential protein expression profile in MUC1-expressing versus Muc1-null cells. A, Western blotting analysis of KCM and KCKO cell lysates probed various proteins. B, proteomics data from KCKO and KCM cell lysates (average $n = 2$ with each experiment conducted in triplicate). Data displayed as fold increase in KCM compared with KCKO cells. Only proteins that were changed more than 2-fold are shown.

had low proliferative index *in vitro* even when supplemented with exogenous growth factors known to enhance tumor cell proliferation (Fig. 3 A–C). Further, MUC1 was shown to regulate cell cycle, as Muc1 deficiency lead to fewer cells entering the G_2–M phase of the cell cycle (Fig. 4B). In addition, MUC1 drove Cdc-25c expression, a tyrosine phosphatase that triggers entry into mitosis. As activated ERK1/2 is known to interact with Cdc-25c during interphase and phosphorylate Cdc-25c during mitosis (18), increased levels of extracellular signal regulated kinase (ERK) activation may be partially

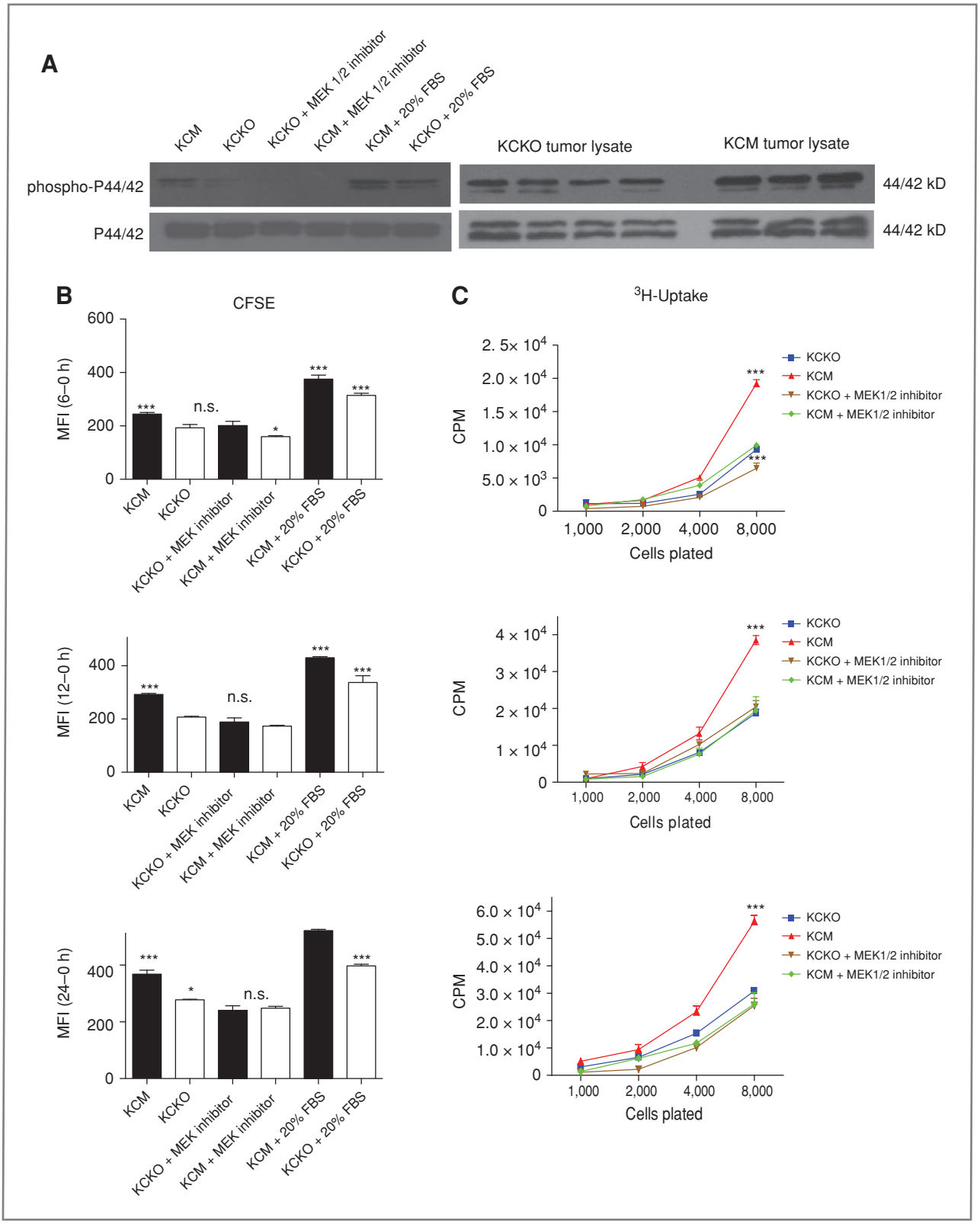

Figure 6. Treatment with MEK1/2 inhibitor, U0126, abrogates proliferation of KCM but not KCKO cells. A, Western blotting analysis showing phosphorylation of MAPK was completely abrogated with the addition of U0126, the MEK1/2 inhibitor (inhib.), B and C, proliferation of KCM and KCKO cells 6, 12, and 24 hours posttreatment with U0126 by using the CFSE dilution assay (B) and [^{3}H]-thymidine uptake assay (C). Experiments were repeated 3 times in triplicate. *, $P < 0.05$; ***, $P < 0.001$; n.s., not significant.

responsible for the upregulation of cdc-25c and thereby enhanced mitosis and entry into the G_2–M phase of the cell cycle. To that effect, treatment with U0126, reduced proliferation of MUC1-expression cells to that of Muc1-null cells (Fig. 6A and B).

MUC1 regulation of cell-cycle checkpoints, proliferation, and invasion could also be attributed to strikingly higher levels of tubulin-α2 chain and nestin proteins (Fig. 5B). Nestin, a marker for proliferating and invading cells, is differentially expressed during the cell cycle and promotes cell proliferation (19, 20). Nestin is also known to interact with Cyclin-dependent kinase 5 (CDK5), a kinase which phosphorylates MEK1. Thus, we hypothesize that MUC1 regulation of nestin may activate CDK5 and thereby enhance phosphorylation of MEK1. Interestingly, inhibition of the ERK pathway has been shown to suppress the expression of nestin (19), once again, making the MAPK/ERK pathway an especially attractive target. Tubulin-α2 is a major constituent of microtubules and is required for mitotic spindle organization, mitosis, growth, and cell migration, thus emphasizing another important role of MUC1 in cell division. Currently, small molecule inhibitors of tubulin are clinically used as antimitotic drugs (21). Importantly, these antimitotic drugs have shown efficacy against multidrug-resistant tumors.

We postulate that the strong oncogenic signaling motifs reside in the cytoplasmic tail of MUC1 (MUC1 CT). MUC1 CT is a transmembrane receptor that is known to function as an oncoprotein (22–24). The tyrosines in MUC1 CT are essential for the oncogenic signal to occur in pancreatic cancer cells (14) and contains a YTNP site that, when phosphorylated, interacts with the proteins of the MAPK pathway (10, 11). Our data and the above findings enable us to postulate that MUC1 contributes to pancreatic cancer cell growth and survival by promoting activation of the MAPK pathway, as pharmaceutically inhibiting this pathways inhibited proliferation in MUC1-expressing cells.

We have previously shown that treatment with a MUC1-based vaccine in combination with celecoxib was extremely effective in halting tumor progression in the KCM mice (12). Furthermore, we have recently shown that the tyrosines in MUC1 CT was essential for epithelial to mesenchymal transition and invasion (14). Thus, targeting MUC1 CT may be an attractive approach, especially because the activation of MAPK pathway in pancreatic cancer cells may occur in part via MUC1 CT phosphorylation and interaction with β-catenin (14).

Disclosure of Potential Conflicts of Interest

No potential conflicts of interest were disclosed.

Acknowledgments

We thank all the technicians in the animal facility for their assistance in maintaining our colonies.

Grant Support

This study was supported by NIH RO1 CA118944-01A1.

The costs of publication of this article were defrayed in part by the payment of page charges. This article must therefore be hereby marked *advertisement* in accordance with 18 U.S.C. Section 1734 solely to indicate this fact.

Received December 8, 2010; revised May 2, 2011; accepted May 4, 2011; published OnlineFirst May 10, 2011.

References

1. Saif MW. Pancreatic cancer: highlights from the 42nd annual meeting of the American Society of Clinical Oncology 2006. JOP 2006;7:337–48.
2. Acres B, Limacher JM. MUC1 as a target antigen for cancer immunotherapy. Expert Rev Vaccines 2005. 4:493–502.
3. Tinder TL, Subramani DB, Basu GD, Bradley JM, Schettini J, Million A, et al. MUC1 enhances tumor progression and contributes toward immunosuppression in a mouse model of spontaneous pancreatic adenocarcinoma. J Immunol 2008;181:3116–25.
4. Levi E, Klimstra DS, Andea A, Basturk O, Adsay NV. MUC1 and MUC2 in pancreatic neoplasia. J Clin Pathol 2004;57:456–62.
5. Chhieng DC, Benson E, Eltoum I, Eloubeidi MA, Jhala N, Jhala D, et al. MUC1 and MUC2 expression in pancreatic ductal carcinoma obtained by fine-needle aspiration. Cancer 2003;99:365–71.
6. Adsay NV, Basturk O, Cheng JD, Andea AA. Ductal neoplasia of the pancreas: nosologic, clinicopathologic, and biologic aspects. Semin Radiat Oncol 2005;15:254–64.
7. Adsay NV, Merati K, Andea A, Sarkar F, Hruban RH, Wilentz RE, et al. The dichotomy in the preinvasive neoplasia to invasive carcinoma sequence in the pancreas: differential expression of MUC1 and MUC2 supports the existence of two separate pathways of carcinogenesis. Mod Pathol 2002;15:1087–95.
8. Moniaux N, Andrianifahanana M, Brand RE, Batra SK. Multiple roles of mucins in pancreatic cancer, a lethal and challenging malignancy. Br J Cancer 2004;91:1633–8.
9. Hingorani SR, Petricoin EF, Maitra A, Rajapakse V, King C, Jacobetz MA, et al. Preinvasive and invasive ductal pancreatic cancer and its early detection in the mouse. Cancer Cell 2003;4: 437–50.
10. Hingorani SR, Petricoin EF, Maitra A, Rajapakse V, King C, Jacobetz MA, et al. Preinvasive and invasive ductal pancreatic cancer and its early detection in the mouse. Cancer Cell 2003; 4:437–450.
11. Adhikary R, Mukherjee P, Krishnamoorthy G, Kunkle RA, Casey TA, Rasmussen MA, et al. Fluorescence spectroscopy of the retina for diagnosis of transmissible spongiform encephalopathies. Anal Chem 2010;82:4097–101.
12. Mukherjee P, Basu GD, Tinder TL, Subramani DB, Bradley JM, Arefayene M, et al. Progression of pancreatic adenocarcinoma is significantly impeded with a combination of vaccine and COX-2 inhibition. J Immunol 2009;182:216–24.
13. Spicer AP, Rowse GJ, Lidner TK, Gendler SJ. Delayed mammary tumor progression in Muc-1 null mice. J Biol Chem 1995;270:30093–101.
14. Roy LD, Sahraei M, Subramani DB, Besmer D, Nath S, Tinder TL, et al. MUC1 enhances invasiveness of pancreatic cancer cells by inducing epithelial to mesenchymal transition. Oncogene 2011; 30:1449–59.
15. Hoang MV, Nagy JA, Senger DR. Cdc42-mediated inhibition of GSK-3beta improves angio-architecture and lumen formation during VEGF-driven pathological angiogenesis. Microvasc Res 2011; 81:34–43.
16. Sheng H, Shao J, Morrow JD, Beauchamp RD, DuBois RN. Modulation of apoptosis and Bcl-2 expression by prostaglandin E2 in human colon cancer cells. Cancer Res 1998;58: 362–6.

17. Sheng H, Shao J, Washington MK, DuBois RN. Prostaglandin E2 increases growth and motility of colorectal carcinoma cells. J Biol Chem 2001;276:18075–81.
18. Wang R, He G, Nelman-Gonzalez M, Ashorn CL, Gallick GE, Stukenberg PT, et al. Regulation of Cdc25C by ERK-MAP kinases during the G2/M transition. Cell 2007;128:1119–32.
19. Kalluri HS, Vemuganti R, Dempsey RJ. Mechanism of insulin-like growth factor I-mediated proliferation of adult neural progenitor cells: role of Akt. Eur J Neurosci 2007;25:1041–8.
20. Wiese C, Rolletschek A, Kania G, Blyszczuk P, Tarasov KV, Tarasova Y, et al. Nestin expression–a property of multi-lineage progenitor cells?Cell Mol Life Sci 2004;61:2510–22.
21. Beckers T, Reissmann T, Schmidt M, Burger AM, Fiebig HH, Vanhoefer U, et al. 2-aroylindoles, a novel class of potent, orally active small molecule tubulin inhibitors. Cancer Res 2002;62:3113–9.
22. Kufe DW. Mucins in cancer: function, prognosis and therapy. Nat Rev Cancer 2009;9:874–85.
23. Gendler SJ. MUC1, the renaissance molecule. J Mammary Gland Biol Neoplasia 2001;6:339–53.
24. Schroeder JA, Masri AA, Adriance MC, Tessier JC, Kotlarczyk KL, Thompson MC, et al. MUC1 overexpression results in mammary gland tumorigenesis and prolonged alveolar differentiation. Oncogene 2004;23:5739–47.